Analytical Expressions for the Power Spectral Density of CP-OFDM and ZP-OFDM Signals

Toon van Waterschoot, Vincent Le Nir, Jonathan Duplicy, *Member, IEEE*, and Marc Moonen, *Fellow, IEEE*

***Abstract*—In this letter, analytical expressions are derived for the power spectral density (PSD) of orthogonal frequency division multiplex (OFDM) signals employing a cyclic prefix (CP-OFDM) or zero padding (ZP-OFDM) time guard interval. Under the relatively weak assumptions that i) the data are independent and identically distributed on all OFDM subcarriers and ii) the OFDM pulse shape is sufficiently localized in time, simple closed-form PSD expressions can be obtained. These expressions are then compared to existing OFDM PSD expressions and validated by inspecting the power spectra of some standardized OFDM signals.**

***Index Terms*—Cyclic prefix (CP), orthogonal frequency division multiplex (OFDM), power spectral density (PSD), zero padding (ZP).**

I. Introduction

ORTHOGONAL frequency division multiplexing (OFDM) has become a widely recognized modulation technique for high-data-rate communication systems. An OFDM signal consists of a number of modulated subcarriers, computed with an inverse discrete Fourier transform (IDFT), which are orthogonal in the absence of a dispersive communication channel. With the aim of compensating for the intersymbol interference (ISI) that may arise in a time-dispersive environment, a time guard interval is inserted between successive OFDM symbols, as obtained at the output of the IDFT modulator. Traditionally, the time guard interval has been defined as a periodic extension of the succeeding OFDM symbol [1], resulting in the well-known cyclic-prefix OFDM (CP-OFDM). In this way, the loss of subcarrier orthogonality in a time-dispersive environment can be annihilated, and hence intercarrier interference (ICI) can be avoided. However, some distinct equalization advantages can be obtained if the time guard interval is padded with zeros [2], resulting in the so-called zero-padding OFDM (ZP-OFDM).

Manuscript received October 31, 2009; revised January 05, 2010. First published January 15, 2010; current version published February 19, 2010. This work was performed at the ESAT Laboratory of Katholieke Universiteit (K.U.) Leuven, in the frame of K.U. Leuven Research Council: CoE EF/05/006 Optimization in Engineering (OPTEC), the Belgian Programme on Interuniversity Attraction Poles initiated by the Belgian Federal Science Policy Office IUAP P6/04 ["Dynamical systems, control and optimization" (DYSCO), 2007–2011], Concerted Research Action GOA-AMBioRICS, and EU/FP7-ICT-2007-1 Project 216785 ["Ultra-wide band real-time interference monitoring and cellular management strategies" (UCELLS)]. The scientific responsibility is assumed by its authors. The associate editor coordinating the review of this manuscript and approving it for publication was Dr. Jian-Kang Zhang.

T. van Waterschoot and M. Moonen are with the Katholieke Universiteit Leuven, ESAT-SCD, B-3001 Leuven, Belgium (e-mail tvanwate@esat.kuleuven.be; moonen@esat.kuleuven.be).

V. Le Nir is with the Royal Military Academy, CISS, B-1000 Brussels, Belgium (e-mail vincent.lenir@rma.ac.be).

J. Duplicy is with SMRD Agilent Technologies, B-3110 Rotselaar, Belgium (e-mail jonathan_duplicy@agilent.com).

Digital Object Identifier 10.1109/LSP.2010.2040651

In this letter, analytical expressions for the power spectral density (PSD) of CP-OFDM and ZP-OFDM signals are derived, which may be useful in a variety of research applications. One of the main motivations for deriving PSD expressions has been the need to predict the in-band and out-of-band radiation produced by OFDM transmitters, so as to guarantee their compliance with regulatory spectrum masks [3]–[9]. More recently, parametric models of the OFDM PSD have been used for blind estimation of the OFDM carrier frequency offset [10] and OFDM modulation parameters [11].

The PSD of an OFDM signal depends on the characteristics of four signal operations performed at the transmitter side: the IDFT modulation, the insertion of the (CP or ZP) time guard interval, the pulse shaping, and the interpolation filtering. Pulse shaping is applied to limit the out-of-band radiation and further reduce the ICI, and is typically realized by means of a time window function applied to the OFDM symbol after the time guard interval has been inserted [8]. On the other hand, the interpolation filter serves to bound the OFDM bandwidth before D/A conversion. Existing OFDM PSD expressions derived in [3]–[9] implicitly rely on the assumption that either rectangular pulse shaping is applied [8], [9] or that the influence of the interpolation filter can be disregarded [3]–[7]. Here, we derive PSD expressions that hold for arbitrary pulse shaping and interpolation filters, under the assumption that: 1) the data are independent and identically distributed (i.i.d.) on all OFDM subcarriers and 2) the pulse shape is sufficiently localized in time (to be defined in Section II). The second assumption indeed holds true for many pulse shapes used in practice, while the first assumption is in practice often violated due to the use of null subcarriers. Nevertheless, this first assumption allows us to derive surprisingly simple PSD expressions which provide an approximation of the in-band PSD that is sufficiently accurate, even when null subcarriers are present, for many practical applications.

The letter is organized as follows. In Section II, we derive a PSD expression that is valid under the two assumptions mentioned earlier, regardless of the type of time guard interval, pulse shaping and interpolation filtering used. This expression is then particularized for CP-OFDM and ZP-OFDM signals, by noting that the CP and ZP time guard interval are merely different pulse shapes. The obtained PSD expressions are validated in Section III by comparing these with existing PSD expressions and inspecting the power spectra of standardized CP-OFDM and ZP-OFDM signals. Finally, Section IV concludes the letter.

II. Derivation of PSD Expressions

In an OFDM transmitter, a discrete-time baseband signal $x[n]$ is generated by IDFT modulation, time guard interval insertion, and pulse shaping (see, e.g., [12])

$$x[n] = \sum_{l=-\infty}^{\infty} \left(\sum_{k=0}^{N-1} c_{k,l} g_{\mathrm{P}}[n - lM] w^{k(n-lM)} \right), \quad n \in \mathbb{Z}. \quad (1)$$

1070-9908/$26.00 © 2010 IEEE

Authorized licensed use limited to: IEEE Xplore. Downloaded on April 09,2010 at 18:23:34 UTC from IEEE Xplore. Restrictions apply.

Here, $w \triangleq e^{j(2\pi/N)}$, n, k, and l denote the discrete time index, the discrete frequency index, and the OFDM symbol index, respectively, N and M denote the number of subcarriers and the symbol length, respectively, $g_{\mathrm{P}}[n]$ denotes the pulse shaping window, and $c_{k,l}$ represents the complex-valued data symbol (taken from a finite alphabet constellation) that is modulated on the kth subcarrier of the lth symbol. Note that we focus here on the baseband representation, i.e., the complex envelope of the real-valued transmitted OFDM signal. An analog signal $x(t)$ is then obtained by feeding the discrete-time baseband signal $x[n]$ to a D/A converter equipped with an interpolation filter $g_{\mathrm{I}}(t)$ [8]

$$x(t) = \sum_{n=-\infty}^{\infty} x[n] g_{\mathrm{I}}(t - nT_s) \tag{2}$$

where T_s denotes the sampling interval employed in the OFDM transmitter and $t \in \mathbb{R}$ represents continuous time.

The PSD of the analog baseband signal $x(t)$ is defined as [13, ch. 6]

$$P_x(f) = \lim_{\mathcal{T}\to\infty} \left(\frac{1}{\mathcal{T}} E\{ |\mathcal{F}\{x_{\mathcal{T}}(t)\}|^2 \} \right) \tag{3}$$

with $E\{\cdot\}$ and $\mathcal{F}\{\cdot\}$ denoting the expectation operator and the Fourier transform operator, respectively, and $x_{\mathcal{T}}(t)$ a truncated version of $x(t)$ in the time interval $(-\mathcal{T}/2, \mathcal{T}/2)$. Existing OFDM PSD expressions [3]–[7], [9] originate from different ways of evaluating the analog baseband signal PSD in (3). However, these are all based on the general result that the PSD of a signal of the form

$$x(t) = \sum_{i=-\infty}^{\infty} a_i f(t - iT) \tag{4}$$

is given by

$$P_x(f) = \frac{|F(f)|^2}{T} \left[R(0) + 2 \sum_{m=1}^{\infty} R(m) \cos(2\pi f m T) \right] \tag{5}$$

where $\{a_i\}_{i=-\infty}^{\infty}$ is a digital data symbol sequence, assumed stationary and hence having an autocorrelation function $R(i,m) = R(m) \triangleq E\{a_i^* a_{i+m}\}$, while $f(t)$ and $F(f)$ represent the time-domain waveform and frequency spectrum of the analog pulse shape, respectively, and T denotes the pulse width [13, ch. 6]. The differences in the evaluation of (3) originate from the fact that, when comparing (1)–(2) and (4), there are different ways of deciding which part of the transmitted signal in (1)–(2) corresponds to the data symbols a_i, and which part corresponds to the pulse shape $f(t)$. Essentially, the expressions derived in [3]–[7] result from the choice $f(t) = g_{\mathrm{P}}(t)$, with $g_{\mathrm{P}}(t)$ obtained from $g_{\mathrm{P}}[n]$ using a perfect (brick-wall) interpolation filter $g_{\mathrm{I}}(t)$. The approach in [9] is based on choosing $f(t) = g_{\mathrm{I}}(t)$ and assuming a rectangular pulse shape $g_{\mathrm{P}}[n]$.

We will evaluate the transmitted baseband signal PSD in (3) using an approach similar to the approach in [9], yet without making strict assumptions on the type of pulse shape used. By defining the mapping

$$a_n = \sum_{l=-\infty}^{\infty} \left(\sum_{k=0}^{N-1} c_{k,l} g_{\mathrm{P}}[n - lM] w^{k(n-lM)} \right) \tag{6}$$

$$f(t) = g_{\mathrm{I}}(t) \tag{7}$$

we obtain from (4)–(5), with $i = n$ and $T = T_s$, that

$$P_x(f) = \frac{|G_i(f)|^2}{T_s} \left[R(0) + 2 \sum_{m=1}^{\infty} R(m) \cos(2\pi f m T_s) \right]. \tag{8}$$

It should be noted that the sequence $\{a_n\}$ as given in (6) is in general a cyclostationary process. In this case, (8) is an expression for the time-averaged PSD with $R(m)$ the time-averaged autocorrelation function of $\{a_n\}$, where time averaging is performed over one cyclic period [9], [14, ch. 6]. In general, we can write the (time-varying) autocorrelation function of $\{a_n\}$ as shown in (9), at the bottom of the page. We will now simplify this expression by making two assumptions.

Assumption 1: If we assume that the data symbols $c_{k,l}$ are i.i.d. for all subcarriers, then it follows that $R(n,m)$ is nonzero only if $k = k'$ and $l = l'$. Moreover, we can exploit the identity

$$\sum_{k=0}^{N-1} w^{km} = \begin{cases} N, & \text{for } m = iN \ (i \in \mathbb{Z}) \\ 0, & \text{for } m \neq iN \ (i \in \mathbb{Z}) \end{cases} \tag{10}$$

to rewrite the autocorrelation function in (9) as shown in (11), at the bottom of the page, where σ_c^2 denotes the variance of the data symbols $c_{k,l}$. Note that a similar result was obtained in [12]. It can be seen from (11) that in general, $R(n,m)$ is a periodic function (with period M) and hence $\{a_n\}$ in (6) is indeed a cyclostationary process.

Assumption 2: If we assume that the pulse shape is sufficiently localized in time, in the sense that $g_{\mathrm{P}}[n] = 0$, $n \notin \{0, \ldots, 2N-1\}$ (which is the case for many pulse shapes that are used in practical OFDM systems), the expression in (11) reduces to

$$R(n,m) = \begin{cases} N\sigma_c^2 \sum_{l=-1}^{1} (g_{\mathrm{P}}[n - lM])^2, & \text{for } m = 0 \\ N\sigma_c^2 g_{\mathrm{P}}[n] g_{\mathrm{P}}[n \pm N], & \text{for } m = \pm N \\ 0, & \text{for } m \neq 0, \pm N \end{cases}$$

and the time-averaged autocorrelation function can then be calculated as

$$R(m) = \begin{cases} \frac{N\sigma_c^2}{M} \sum_{n=0}^{2N-1} (g_{\mathrm{P}}[n])^2, & \text{for } m = 0 \\ \frac{N\sigma_c^2}{M} \sum_{n=N}^{M-1} g_{\mathrm{P}}[n] g_{\mathrm{P}}[n-N], & \text{for } m = \pm N \\ 0, & \text{for } m \neq 0, \pm N. \end{cases} \tag{12}$$

$$R(n,m) = E\left\{ \left[\sum_{l=-\infty}^{\infty} \left(\sum_{k=0}^{N-1} c_{k,l}^* g_{\mathrm{P}}[n - lM] w^{-k(n-lM)} \right) \right] \times \left[\sum_{l'=-\infty}^{\infty} \left(\sum_{k'=0}^{N-1} c_{k',l'} g_{\mathrm{P}}[n + m - l'M] w^{k'(n+m-l'M)} \right) \right] \right\}. \tag{9}$$

$$R(n,m) = \begin{cases} N\sigma_c^2 \sum_{l=-\infty}^{\infty} g_{\mathrm{P}}[n - lM] g_{\mathrm{P}}[n + iN - lM], & \text{for } m = iN \ (i \in \mathbb{Z}) \\ 0, & \text{for } m \neq iN \ (i \in \mathbb{Z}) \end{cases} \tag{11}$$

Authorized licensed use limited to: IEEE Xplore. Downloaded on April 09,2010 at 18:23:34 UTC from IEEE Xplore. Restrictions apply.

We can now combine (8) and (12) to obtain an analytical expression for the analog baseband signal PSD that is generally applicable under the two assumptions mentioned above, and which is given in (13), shown at the bottom of the page, where the subcarrier separation is defined as $\Delta_f = 1/(NT_s)$. This essentially means that, within the bandwidth of the interpolation filter, the PSD of an OFDM signal behaves as a cosine function w.r.t. frequency, with the cosine maxima occuring at the subcarrier frequencies (and beyond).

The result in (13) is valid regardless of the type of time guard interval (CP or ZP). However, in case of a ZP time guard interval, the insertion of $M-N$ zeros between successive OFDM symbols is equivalent to using a pulse shape that spans only N samples, i.e., $g_{\mathrm{P}}[n] = 0,\ n \notin \{0, \ldots, N-1\}$. Hence, the PSD expression in (13) can be simplified to

$$P_x^{(\mathrm{ZP})}(f) = \frac{N|\sigma_c G_i(f)|^2}{MT_s} \sum_{n=0}^{N-1} (g_{\mathrm{P}}[n])^2. \tag{14}$$

III. Validation of PSD Expressions

A. Comparison With Existing PSD Expressions

Most existing PSD expressions are derived by summing the power spectra of individual subcarriers, under the assumption that the data at each subcarrier are statistically independent and mutually orthogonal [6]. This leads to the general PSD expression found in [5]–[8], [10]

$$P_x(f) = \frac{\sigma_c^2}{MT_s} \sum_{k=0}^{N-1} |G_p[(f-k\Delta_f)MT_s]|^2 \tag{15}$$

and to the specific PSD expressions found in [3]–[5], [7] for the case when rectangular pulse shaping is applied

$$P_x(f) = \frac{\sigma_c^2}{MT_s} \sum_{k=0}^{N-1} (\mathrm{sinc}[(f-k\Delta_f)MT_s])^2 \tag{16}$$

where $\mathrm{sinc}(\alpha) \triangleq \sin(\pi\alpha)/(\pi\alpha)$. As pointed out in [8], (16) provides an approximation to the true PSD. Indeed, the spectrum of a sampled rectangular window is not a sinc function, but rather a periodic sinc function, defined as

$$\mathrm{sinc}_M(\alpha) = \begin{cases} (-1)^{\alpha(M-1)}, & \text{for } \alpha \in \mathbb{Z} \\ \dfrac{\sin(\pi M\alpha)}{M\sin(\pi\alpha)}, & \text{for } \alpha \notin \mathbb{Z}. \end{cases} \tag{17}$$

As a consequence, the expression in (16) is only valid in the limiting case when $T_s \to 0$, which explains why interpolation filtering is disregarded in [3]–[7]. For the more realistic case when $T_s \neq 0$, the influence of the interpolation filter $g_{\mathrm{I}}(t)$ should be taken into account, which leads to the alternative PSD expression found in [8]

$$P_x(f) = \frac{|\sigma_c G_i(f)|^2}{MT_s} \sum_{k=0}^{N-1} (M\mathrm{sinc}_M[(f-k\Delta_f)T_s])^2. \tag{18}$$

The equivalence between the PSD expressions in (13) and (18) can be shown by using the PSD expression derived in [10] as an intermediate result. By exploiting the fact that the autocorrelation function of a sampled rectangular window is a sampled triangular function, it is straightforward to show that the expression in (18) is equivalent to the expression found in [10], in which the interpolation filter $g_{\mathrm{I}}(t)$ is implicitly assumed to be a perfect (brick-wall) filter

$$P_x(f) = \frac{\sigma_c^2}{MT_s} \sum_{k=0}^{N-1} \left(\sum_{m=-M+1}^{M-1} (M-|m|)\cos[2\pi f_{k,m}] \right) \tag{19}$$

with $f_{k,m} \triangleq (f - k\Delta_f)mT_s$. By changing the order of the summations in (19), the expression in (19) can be rewritten, using the identity in (10), as

$$P_x(f) = \frac{N\sigma_c^2}{MT_s} \left[M + 2(M-N)\cos\left(\frac{2\pi f}{\Delta_f}\right) \right] \tag{20}$$

which is obviously equivalent to (13) in case of a rectangular pulse shape and a perfect (brick-wall) interpolation filter.

B. Example Power Spectra of Standardized OFDM Signals

1) Example 1—IEEE 802.11a WLAN Signal: Two WLAN OFDM signals have been simulated with specifications taken from the IEEE 802.11a standard [15], i.e., $N = 64$ subcarriers with a 16-QAM modulation on each subcarrier, a CP time guard interval of 16 samples (resulting in a symbol length of $M = 80$ samples), and a bandwidth of $f_s = 20$ MHz. Pulse shaping is performed with a time-domain window as suggested in [15, Sec. 17.3.2.5] and a 20th-order linear-phase finite impulse response (FIR) interpolation filter $g_{\mathrm{I}}(t)$ is used. The first WLAN signal has no null subcarriers, while the second WLAN signal has one null subcarrier at dc and 11 null subcarriers at the band edges, as specified in [15, Sec.17.3.2.5]. The PSD of these signals has been estimated using the averaged periodogram technique, where averaging is performed over 1000 OFDM symbols. These PSD estimates are shown in Fig. 1(a), together with the PSD curve obtained by evaluating the analytical expression in (13) using the given signal specifications. A zoom on the upper band edge of the WLAN PSD curves is displayed in Fig. 1(b). From these figures, it can be seen that the PSD curve corresponding to the analytical expression in (13) closely follows the estimated PSD curve for the simulated signal without null subcarriers. The estimated PSD curve for the simulated signal with null subcarriers corresponds remarkably well to the analytical PSD curve, except in the frequency region where the null subcarriers are located.

2) Example 2—ECMA-368 UWB Signal: Again, two OFDM signals have been simulated with and without null subcarriers, yet with the signal specifications taken from the ECMA-368 UWB standard [16]. These signals have $N = 128$ QPSK-modulated subcarriers, of which the dc subcarrier and the outer five subcarriers are fixed to null in the second OFDM signal, as specified in [16, Sec. 10.10.1]. The time guard interval is in this case a ZP interval of 37 samples, such that the symbol length $M = 165$, and the bandwidth equals $f_s = 528$ MHz. The pulse shape $g_{\mathrm{P}}[n]$ corresponds to a length-N sampled rectangular window, and the interpolation filter is again a 20th-order linear-phase FIR filter.

$$P_x(f) = \frac{N|\sigma_c G_i(f)|^2}{MT_s} \left[\sum_{n=0}^{2N-1} (g_{\mathrm{P}}[n])^2 + 2\cos\left(\frac{2\pi f}{\Delta_f}\right) \sum_{n=N}^{M-1} g_{\mathrm{P}}[n] g_{\mathrm{P}}[n-N] \right] \tag{13}$$

Authorized licensed use limited to: IEEE Xplore. Downloaded on April 09,2010 at 18:23:34 UTC from IEEE Xplore. Restrictions apply.

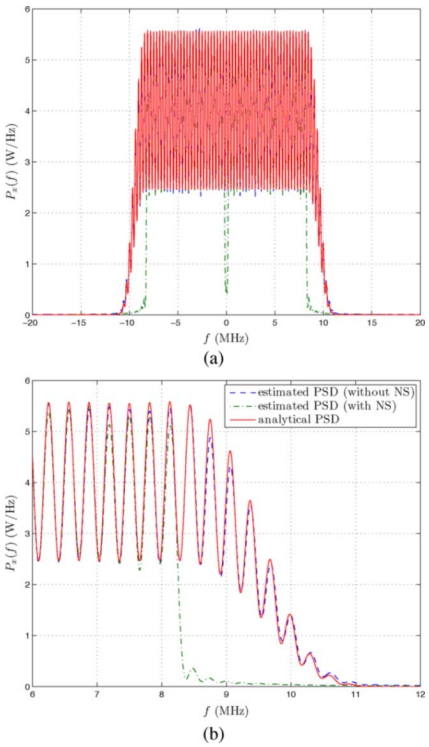

Fig. 1. Example 1: PSD curves for IEEE 802.11a WLAN signal: (a) full view and (b) zoom on upper band edge (NS = null subcarriers).

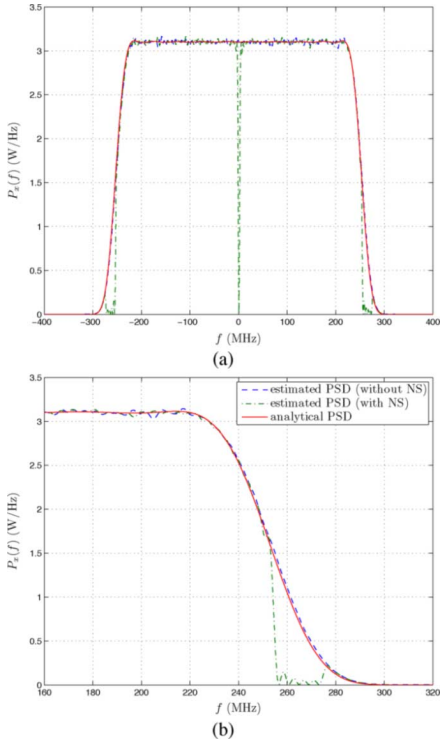

Fig. 2. Example 2: PSD curves for ECMA-368 UWB signal: (a) full view and (b) zoom on upper band edge (NS = null subcarriers).

The PSD curves for the UWB OFDM signals are shown in Fig. 2(a) and (b). Here also there is a clear correspondence between the analytical PSD curve and the estimated PSD curves without null subcarriers and with null subcarriers, outside of the null subcarriers frequency region.

IV. Conclusion

In this letter, we have proposed simple yet accurate analytical expressions for the PSD of CP-OFDM and ZP-OFDM signals, which explicitly depend on the pulse shape and interpolation filter characteristics, and are based on two assumptions. While the second assumption on the time localization of the pulse shape is valid for many standardized OFDM signals, the first assumption on the independent and identical distribution of the subcarrier data is often violated due to the use of null subcarriers. However, from simulation examples it appears that even in the presence of null subcarriers, the analytical PSD expressions provide a remarkably good approximation to the PSD estimated from the OFDM data.

References

[1] A. Peled and A. Ruiz, "Frequency domain data transmission using reduced computational complexity algorithms," in *Proc. IEEE Int. Conf. Acoustics, Speech, Signal Processing (ICASSP'80)*, Denver, CO, Apr. 1980, vol. 5, pp. 964–967.

[2] G. B. Giannakis, "Filterbanks for blind channel identification and equalization," *IEEE Signal Process. Lett.*, vol. 4, no. 6, pp. 184–187, Jun. 1997.

[3] M. Pauli and H.-P. Kuchenbecker, "On the reduction of the out-of-band radiation of OFDM-signals," in *Conf. Rec. 1998 IEEE Int. Conf. Commun. (ICC'98)*, Atlanta, GA, Jun. 1998, vol. 3, pp. 1304–1308.

[4] Y. Zhao, "In-band and out-band spectrum analysis of OFDM communication systems using ICI cancellation methods," in *Proc. 2000 Int. Conf. Communication Technology (WCC-ICCT'00)*, Beijing, China, Aug. 2000, vol. 1, pp. 773–776.

[5] A. D. S. Jayalath and C. Tellambura, "Reducing the out-of-band radiation of OFDM using an extended guard interval," in *Proc. IEEE VTS 54th Vehicular Technology Conf. (VTC'01 Fall)*, Atlantic City, NJ, Oct. 2001, vol. 2, pp. 829–833.

[6] C. Liu and F. Li, "Spectrum modelling of OFDM signals for WLAN," *Electron. Lett.*, vol. 40, no. 22, pp. 1431–1432, Oct. 2004.

[7] C. Liu and F. Li, "On spectrum modeling of OFDM signals for digital broadcasting," in *Proc. 7th Int. Conf. Signal Processing (ICSP'04)*, Beijing, China, Sep. 2004, vol. 3, pp. 1886–1889.

[8] G. Cuypers, K. Vanbleu, G. Ysebaert, and M. Moonen, "Intra-symbol windowing for egress reduction in DMT transmitters," *EURASIP J. Appl. Signal Process.*, vol. 2006, Article ID 70387.

[9] M. T. Ivrlač and J. A. Nossek, "Influence of a cyclic prefix on the spectral power density of cyclo-stationary random sequences," in *Multi-Carrier Spread Spectrum 2007*. Dordrecht, The Netherlands: Springer, 2007, vol. 1, pp. 37–46.

[10] S. L. Talbot and B. Farhang-Boroujeny, "Spectral method of blind carrier tracking for OFDM," *IEEE Trans. Signal Process.*, vol. 56, no. 7, pp. 2706–2717, Jul. 2008.

[11] V. Le Nir, T. van Waterschoot, M. Moonen, and J. Duplicy, "Blind CP-OFDM and ZP-OFDM parameter estimation in frequency selective channels," *EURASIP J. Wireless Commun. Networking*, vol. 2009, Article ID 315765.

[12] H. Bölcskei, "Blind estimation of symbol timing and carrier frequency offset in wireless OFDM systems," *IEEE Trans. Commun.*, vol. 49, no. 6, pp. 988–999, Jun. 2001.

[13] L. W. Couch II, *Digital and Analog Communication Systems*. Upper Saddle River, NJ: Prentice-Hall, 1997.

[14] J. G. Proakis, *Digital Communications*. New York: McGraw-Hill, 2001.

[15] *Wireless LAN Medium Access Control (MAC) and Physical Layer (PHY) Specifications: High-Speed Physical Layer in the 5 GHz Band*, IEEE Std. 802.11a-1999(R2003), Sep. 1999.

[16] *High Rate Ultra Wideband PHY and MAC Standard*, ECMA Std. 368, Dec. 2005.

Authorized licensed use limited to: IEEE Xplore. Downloaded on April 09,2010 at 18:23:34 UTC from IEEE Xplore. Restrictions apply.